

---

# UNSUPERVISED POINT CLOUD REGISTRATION VIA SALIENT POINTS ANALYSIS (SPA)

---

A PREPRINT

**Pranav Kadam**

Media Communications Lab  
University of Southern California  
Los Angeles, CA, USA  
pranavka@usc.edu

**Min Zhang**

Media Communications Lab  
University of Southern California  
Los Angeles, CA, USA  
zhan980@usc.edu

**Shan Liu\***

Tencent Media Lab  
Tencent America  
Palo Alto, CA, USA  
shanl@tencent.com

**C.-C. Jay Kuo**

Media Communications Lab  
University of Southern California  
Los Angeles, CA, USA  
cckuo@sipi.usc.edu

September 4, 2020

## ABSTRACT

An unsupervised point cloud registration method, called salient points analysis (SPA), is proposed in this work. The proposed SPA method can register two point clouds effectively using only a small subset of salient points. It first applies the PointHop++ method to point clouds, finds corresponding salient points in two point clouds based on the local surface characteristics of points and performs registration by matching the corresponding salient points. The SPA method offers several advantages over the recent deep learning based solutions for registration. Deep learning methods such as PointNetLK and DCP train end-to-end networks and rely on full supervision (namely, ground truth transformation matrix and class label). In contrast, the SPA is completely unsupervised. Furthermore, SPA's training time and model size are much less. The effectiveness of the SPA method is demonstrated by experiments on seen and unseen classes and noisy point clouds from the ModelNet-40 dataset.

**Keywords** Point cloud registration · PointHop++ · unsupervised machine learning

## 1 Introduction

Point cloud registration refers to the task of finding a spatial transformation that aligns two point cloud sets. Spatial transformation can be rigid (e.g., rotation or translation) or non-rigid (e.g., scaling or non-linear mappings). Reference and transformed point clouds are called the *target* and the *source*, respectively. The goal of registration is to find a transformation that aligns the source with the target.

Point cloud registration has gained popularity with proliferation of 3D scanning devices like LIDAR and its emerging applications in robotics, graphics, mapping, etc. Registration is needed to merge data from different sensors to obtain a globally consistent view, mapping a new observation to known data, etc. Registration is challenging due to several reasons. The source and the target point clouds may have different sampling densities and different number of points. Point clouds may contain outliers and/or be corrupted by noise. Sometimes, only partial views are available.

With the rich deep learning literature in 2D vision, a natural inclination for 3D vision researchers is to develop deep learning methods for point cloud processing nowadays. These solutions are heavily supervised and trained end-to-end.

---

\*This work was supported by Tencent Media Lab.

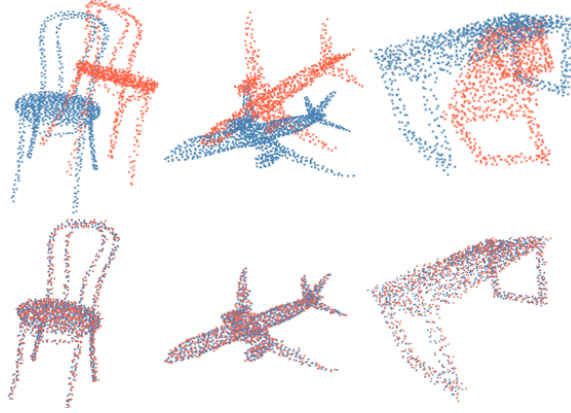


Figure 1: Registration of noisy point clouds (in orange) with noiseless point clouds (in blue) from ModelNet-40 dataset [1] using the SPA method, where the first row is the input and the second row is the output.

Our method offers a contrasting difference – it does not demand ground truth transformation matrix and/or class label for training. It is totally unsupervised. We develop a novel solution, called the Salient Points Analysis (SPA), that exploits local surface properties in selecting a set of salient points. This small subset of points are representative and can be used to estimate the rotation and translation of the entire point cloud set effectively and accurately (see examples in Fig. 1). The performance of the SPA method will be demonstrated by experiments on seen and unseen classes and noisy point clouds from the ModelNet-40 dataset.

The rest of this paper is organized as follows. Related work is reviewed in Sec. 2. The SPA method is described in detail in Sec. 3. Experimental results are reported in Sec. 4. Finally, concluding remarks are given in Sec. 5.

## 2 Related Work

The problem of registration (or alignment) has been studied for a long while. Prior to point cloud processing, the focus has been on aligning lines, parametric curves and surfaces. Traditional methods rely on the spatial coordinates of points. Recent methods adopt feature-based or learning-based approach.

**Classic Methods.** One classic algorithm for point cloud registration is the Iterative Closest Point (ICP) method [2]. The ICP alternates between establishing point correspondences and estimating the transformation. For every point in the source, a matching point in the target is found to minimize the Euclidean distance between the two in the 3D space. Once the point correspondences are established, the rotation matrix that minimizes the point-wise mean square error can be computed using the singular value decomposition (SVD). The ICP is slow and prone to local optima. It works well for only a small degree of rotation. Several variants of ICP were proposed later to address some of the drawbacks such as the globally optimum ICP (Go-ICP) [3] and the fast global registration (FGR) [4].

**Deep Learning Methods.** PointNet [5] was the first deep network developed for point cloud classification and segmentation tasks. PointNetLK [6] uses the PointNet to learn the feature vector from source/target point clouds and then finds the transformation in an iterative manner based on the Lucas and Kanade (LK) algorithm [7]. The Deep Closest Point (DCP) method [8] uses a combination of local and global point features followed by a transformer network. The transformer uses an attention mechanism to enable source/target point cloud features to learn more contextual information. Then, a pointer network is used to find point correspondences. Finally, the SVD is used to estimate the transformation. The DCP uses point-wise features. It is different from a feature vector for the whole point cloud adopted by PointNetLK. Yet, both are fully supervised and trained in an end-to-end manner. Also, they both demand a long training time and a large model size. Our SPA method is much more favorable in all three aspects.

**PointHop and PointHop++.** An explainable point cloud classification called PointHop was proposed in [9]. It consists of multiple PointHop units in cascade. Each PointHop unit constructs a vector of local attributes for every point in the point cloud. A set of nearest neighbors of each point in the 3D space is retrieved, and the 3D space is partitioned into eight octants centered around the point under consideration. The centroid of input point attributes in each octant is computed. The eight centroids are concatenated to form a new attribute vector. The Saab transform [10] is used to reduce the dimension of the attribute vector. Since features of different channels at the output of the Saab transform are uncorrelated, we can decouple them for separable transforms, leading to a more effective transform called the

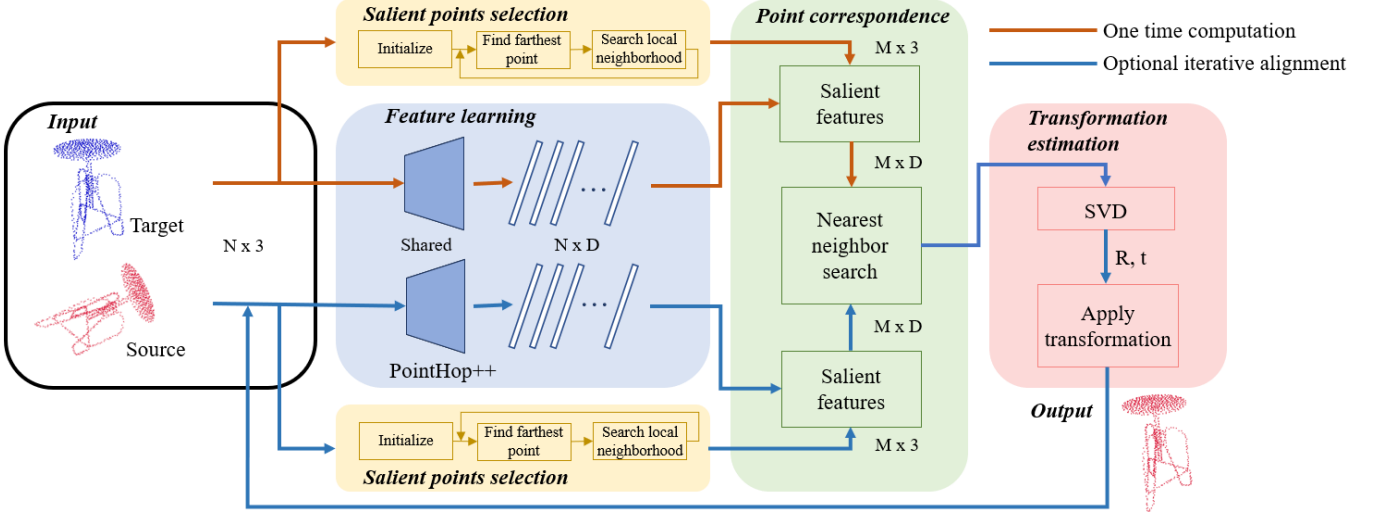


Figure 2: The system diagram of the proposed SPA method.

channel-wise (*c/w*) Saab transform. The *c/w* Saab transform is adopted by PointHop++ [11], which is an enhanced version of PointHop. Both PointHop and PointHop++ use the successive subspace learning (SSL) principle [12] to derive features in an unsupervised manner. PointHop++ will be adopted in the proposed SPA method for feature learning.

### 3 Proposed SPA Method

Let  $X \in \mathbb{R}^3$  and  $Y \in \mathbb{R}^3$  be the target and the source point clouds.  $Y$  is obtained from  $X$  through rotation and translation, which are represented by rotation matrix,  $R_{XY} \in SO(3)$ , and the translation vector,  $t_{XY} \in \mathbb{R}^3$ . Given  $X$  and  $Y$ , the goal is to find the optimal rotation  $R_{XY}^*$  and translation  $t_{XY}^*$  for  $X$  so that they minimize the point-wise mean squared error between transformed  $X$  and  $Y$ . The error term can be written as

$$E(R_{XY}, t_{XY}) = \frac{1}{N} \sum_{i=0}^{N-1} \|R_{XY}^* x_i + t_{XY}^* - y_i\|^2. \quad (1)$$

For simplicity,  $X$  and  $Y$  are assumed to have the same number of points, which is denoted by  $N$ . If the source and target point clouds have a different number of points, only their common points would be considered in computing the error.

The system diagram of the proposed SPA method is shown in Fig. 2. The target and the source point clouds are fed into PointHop++ [11] to learn features. The output for each point is a  $D$ -dimensional feature vector. The salient points selection module selects  $M$  salient points from the set of  $N$  points. Features of the  $M$  salient points are used to find point correspondences using the nearest neighbor search. Finally, SVD is used to estimate the transformation. The output point cloud can be used as the new source for iterative alignment. Yet, the training of PointHop++ is done only once. We will elaborate each module below.

**Feature Learning.** The target and the source point clouds are fed into the same PointHop++ to learn features for every point. We use target point clouds from the training dataset to obtain Module I of PointHop++ using a statistical approach. The training process is same as that in [11]. We should emphasize that Modules II and III of PointHop++ are removed in our current system. They include: feature aggregation and classifier. Cross-entropy-based feature selection is also removed. These removed components are related to the classification but not the registration task. As a result, feature learning with PointHop++ is completely unsupervised. Features from four PointHop units are concatenated to get the final feature vector. The feature dimension depends on energy thresholds chosen in PointHop++ design. We will demonstrate that our method can generalize well on unseen data and unseen classes in Sec. 4.

**Salient Points Selection.** The Farthest Point Sampling (FPS) technique is used in PointHop++ to downsample the point cloud. It offers several advantages for classification such as reduced computation and rapid coverage of the point cloud set. However, FPS is not ideal for registration as it leads to different points being sampled from the target and the source point clouds. We propose a novel method to select a subset of salient points based on the local geometry

information. The new method has a higher assurance that selected points be the same ones sampled from the source and the target. It is detailed below.

We apply the Principal Component Analysis (PCA) to the  $(x, y, z)$  coordinates of points of a local neighborhood which is centered at every point. There are  $N$  points. Thus, it defines  $N$  local neighbors and we conduct the PCA  $N$  times. Mathematically, let  $p_{i,1}, p_{i,2}, \dots, p_{i,K}$  be the  $K$  nearest neighbors of  $p_i$ . The input to this local PCA is  $K$  3D coordinate vectors. We obtain a  $3 \times 3$  covariance matrix that has three eigenvectors and three associated non-negative eigenvalues. We pay attention to the smallest eigenvalue among the three and denote it with  $\lambda_i$ , which is the energy of the third principal component of the local PCA at point  $p_i$ .

Before proceeding, it is worthwhile to give an intuitive explanation to this quantity. Points lying on a flat surface can be well represented by two coordinates in the transformed domain so that the energy of its third component,  $\lambda_i$ , is zero or close to zero. For points lying on edges between surfaces, corners or distinct local regions, they have a large  $\lambda_i$  value. These are salient point candidates since they are more discriminative. Thus, we rank order all points based on their energy values of the third principal component from the largest to the smallest. The point with the largest energy  $\lambda$  is initialized as the first salient point

$$m_0 = p_i, \text{ s.t. } i = \operatorname{argmax}_j(\lambda_j) \quad (2)$$

If we select  $M$  points simply based on the rank order of  $\lambda_i$ , we may end up selecting many points from the same region of largest curvatures. Yet, we need salient points that span the entire point cloud. For this reason, we use the FPS to find the farthest region that contain salient point candidates. In this new region, we again look for the point which has the largest  $\lambda_i$ . To be more exact, we consider two factors jointly: 1) selecting the point according to the order of the  $\lambda_i$  value, and 2) selecting the point that has the largest distance from the set of previously selected points. This process is repeated until  $M$  salient points are determined. Several examples of salient points selected by our method are shown in Fig. 3.



Figure 3:  $M$  salient points (with  $M = 32$ ) of several point cloud sets selected by our algorithm are highlighted.

**Point Correspondence and Transformation Estimation.** We get  $M$  salient points from the target and source. Also, we obtain their features from PointHop++ to establish point correspondences. For each selected salient point in the target point cloud, we use the nearest neighbor search technique in the feature space to find its matched point in the source point cloud. The proximity is measured in terms of the Euclidean distance between the correspondence pair. Finally, we can form a pair of points,  $(q_m, q'_m)$ , of the  $m$ -th matched pair.

Once we have the ordered pairs, the next task is to estimate the rotation matrix and translation vector that best aligns the two point clouds. We revisit Eq. (1), which gives the optimization criterion. A closed-form solution, which minimizes the mean-squared-error (MSE), can be obtained by SVD. The step is summarized below. First, we find centroids of two point clouds as

$$\bar{x} = \frac{1}{N} \sum_{i=0}^{N-1} x_i, \quad \bar{y} = \frac{1}{N} \sum_{i=0}^{N-1} y_i. \quad (3)$$

Then, the covariance matrix is computed via

$$\operatorname{Cov}(X, Y) = \sum_{i=0}^{N-1} (x_i - \bar{x})(y_i - \bar{y})^T. \quad (4)$$

Then, the covariance matrix can be decomposed in form of  $\operatorname{Cov}(X, Y) = USV^T$  via SVD, where  $U$  is the matrix of left singular vectors,  $S$  is the diagonal matrix containing singular values and  $V$  is the matrix of right singular vectors. Then, the optimal rotation matrix  $R_{XY}^*$  and translation vector  $t_{XY}^*$  are given by [13] as

$$R_{XY}^* = UV^T, \quad t_{XY}^* = -R_{XY}^* \bar{x} + \bar{y}. \quad (5)$$

Then, we can align the source point cloud to the target using this transformation. Optionally, we can use an iterative alignment method where the aligned point cloud at the  $i^{th}$  iteration is used as the new *source* for the  $(i + 1)^{th}$  iteration. Even with the iteration, PointHop++ is only trained once.

## 4 Experiments

We use the ModelNet-40 [1] dataset in all experiments. It has 40 object classes, 9,843 training samples and 2,468 test samples. Each point cloud sample consists of 2048 points. Only 1024 points are used in the training. Evaluation metrics include: the Mean Squared Error (MSE), the Root Mean Squared Error (RMSE) and the Mean Absolute Error (MAE) for rotation angles against the X, Y and Z axes in degrees and the translation vector. To train PointHop++, we set the numbers of nearest neighbors to 32, 8, 8, 8 in Hops #1, #2, #3 and #4, respectively. The energy threshold of PointHop++ is set to 0.0001. The following three sets of experiments are conducted.

**Experiment #1: Unseen point clouds.** We train PointHop++ on the target point clouds with training samples from all 40 classes for feature learning. Then, we apply the SPA method to test samples for the registration task. In the experiment, we vary the maximum rotation angles against three axes from  $5^\circ$  to  $60^\circ$  in steps of  $5^\circ$ . For each case, the three angles are uniformly sampled between  $0^\circ$  and the maximum angle. Translation along three axes is uniformly distributed in  $[-0.5, 0.5]$ . We select 32 salient points for SPA. We replace the salient points selection method in SPA with *random* selection and *farthest points* selection while keeping the rest of the procedure the same for performance comparison. We also compare the SPA method with ICP. For fair comparison, every point cloud undergoes exactly the same transformation for all four benchmarking methods. The mean absolute registration errors are plotted as a function of the maximum rotation angle in Fig. 4, where the results after the first iteration are shown. We see from Fig. 4 that the SPA method outperforms the other three methods by a clear margin. Random selection gives the worst results. Interestingly, SPA with farthest sampled points works better than ICP for larger angles. The translation error of all three SPA variants is much less than that of ICP. This validates the effectiveness of the proposed SPA method in global registration.

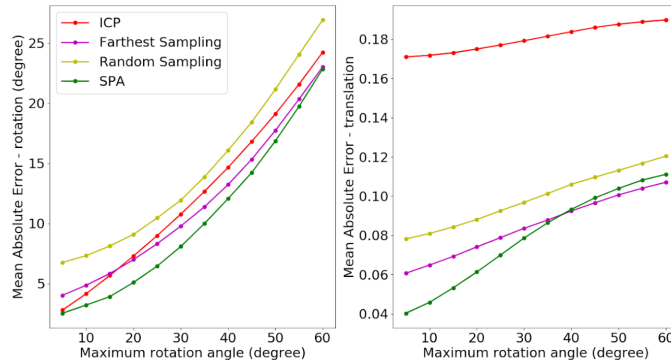


Figure 4: Comparison of the mean absolute registration errors of rotation and translation for four benchmarking methods as a function of the maximum rotation angle on unseen point clouds.

**Experiment #2: Unseen classes.** This experiment is used to study the generalizability of SPA. We adopt the same setup as that in [8] here. We use target point clouds from the first 20 classes of the ModelNet-40 for feature learning in the training phase. Source and target point clouds from remaining 20 classes are used for registration in the testing phase. Rotation angles and the translation are uniformly sampled from  $[0^\circ, 45^\circ]$  and  $[-0.5, 0.5]$ , respectively. We apply SPA for 10 iterations. The results are shown in Table 1. We see that SPA generalizes well on categories that it did not see during training. SPA outperforms ICP by a significant margin. SPA and PointNetLK have comparable performance. Although SPA is still inferior to DCP, the difference between their mean absolute rotation errors is less than  $4^\circ$  while the difference between translation errors is 0.00062.

**Experiment #3: Noisy point clouds.** The objective is to understand the error-resilience property of SPA against noisy input point cloud data. We train PointHop++ on the noiseless target point clouds from all 40 classes for feature learning. In the testing phase, we add independent zero-mean Gaussian noise of variance 0.01 to the three coordinates of each point. Rotation and translation are uniformly sampled from  $[0^\circ, 45^\circ]$  and  $[-0.5, 0.5]$ , respectively. The results are shown in Table 1. Again, we see that SPA outperforms ICP, has comparable performance with PointNetLK and is inferior to DCP. Overall, SPA is robust to additive Gaussian noise.

Method	Registration errors on unseen classes						Registration errors on noisy input point clouds					
	MSE (R)	RMSE (R)	MAE (R)	MSE (t)	RMSE (t)	MAE (t)	MSE (R)	RMSE (R)	MAE (R)	MSE (t)	RMSE (t)	MAE (t)
ICP [2]	467.37	21.62	17.87	0.049722	0.222831	0.186243	558.38	23.63	19.12	0.058166	0.241178	0.206283
PointNetLK [6]	306.32	17.50	5.28	0.000784	0.028007	0.007203	256.16	16.00	4.60	0.000465	0.021558	0.005652
DCP [8]	19.20	4.38	2.68	0.000025	0.004950	0.003597	6.93	2.63	1.52	0.000003	0.001801	0.001697
SPA	354.57	18.83	6.97	0.000026	0.005120	0.004211	331.73	18.21	6.28	0.000462	0.021511	0.004100

Table 1: Registration performance comparison on ModelNet-40 with respect to unseen classes (left) and noisy input point clouds (right).

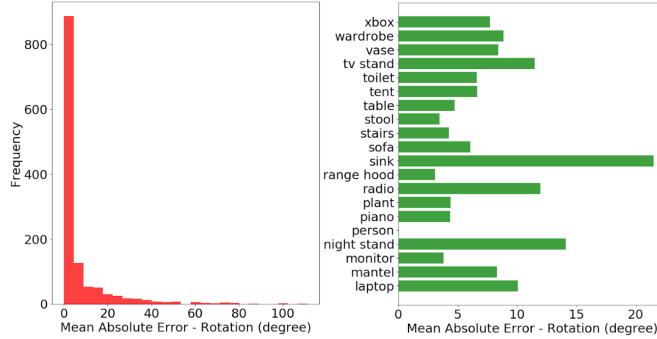


Figure 5: Histogram of mean absolute rotation error for experiment #2 (left) and class-wise error distribution (right)

**Error Analysis.** It is worthwhile to examine the error distribution of the test data as the evaluation metrics provide only an average measure of the performance. We plot the histogram of the MAE(R) for experiment #2 in Fig. 5. It is clear that a large number of point clouds align well with a very small error. Precisely, 38% of the test samples have their MAE(R) less than 1° and 72% of them have their MAE(R) less than 5°.

Also, in Fig. 5 we plot the class-wise MAE(R) for the 20 unseen classes that are not used during training. 8 out of 20 classes have MAE less than 5°. The error is almost 0° for the *person* class.

**Comparison of Model Size and Training Complexity.** The model size of SPA is only 64kB while that of DCP is 21MB. PointNetLK trains PointNet for the classification task first, uses its weights as the initialization and then trains the registration network using a new loss function. Both PointNetLK and DCP demand GPU resources to speed up training. However, in SPA training, CPUs are sufficient and the training time is less than 30 minutes. Apparently, SPA offers a good tradeoff between the model size, computation complexity and registration performance.

## 5 Conclusion and Future Work

An unsupervised point cloud registration method called Salient Points Analysis (SPA) was proposed in this work. The SPA method successfully registers two point clouds with only pairs of discriminative points. The pairing is achieved by the shortest distance in the feature domain learned via PointHop++. The SPA method offers comparable performance as state-of-the-art deep learning methods at a much smaller model size with much less training cost. It is worthwhile to conduct more thorough error analysis for further performance improvement of the SPA method.

## References

- [1] Zhirong Wu, Shuran Song, Aditya Khosla, Fisher Yu, Linguang Zhang, Xiaoou Tang, and Jianxiong Xiao. 3d shapenets: A deep representation for volumetric shapes. In *Proceedings of the IEEE conference on computer vision and pattern recognition*, pages 1912–1920, 2015.
- [2] Paul J Besl and Neil D McKay. Method for registration of 3-d shapes. In *Sensor fusion IV: control paradigms and data structures*, volume 1611, pages 586–606. International Society for Optics and Photonics, 1992.
- [3] Jiaolong Yang, Hongdong Li, Dylan Campbell, and Yunde Jia. Go-icp: A globally optimal solution to 3d icp point-set registration. *IEEE transactions on pattern analysis and machine intelligence*, 38(11):2241–2254, 2015.
- [4] Qian-Yi Zhou, Jaesik Park, and Vladlen Koltun. Fast global registration. In *European Conference on Computer Vision*, pages 766–782. Springer, 2016.

- [5] Charles R Qi, Hao Su, Kaichun Mo, and Leonidas J Guibas. Pointnet: Deep learning on point sets for 3d classification and segmentation. In *Proceedings of the IEEE Conference on Computer Vision and Pattern Recognition*, pages 652–660, 2017.
- [6] Yasuhiro Aoki, Hunter Goforth, Rangaprasad Arun Srivatsan, and Simon Lucey. Pointnetlk: Robust & efficient point cloud registration using pointnet. In *Proceedings of the IEEE Conference on Computer Vision and Pattern Recognition*, pages 7163–7172, 2019.
- [7] Bruce D Lucas, Takeo Kanade, et al. An iterative image registration technique with an application to stereo vision. 1981.
- [8] Yue Wang and Justin M Solomon. Deep closest point: Learning representations for point cloud registration. In *Proceedings of the IEEE International Conference on Computer Vision*, pages 3523–3532, 2019.
- [9] Min Zhang, Haoxuan You, Pranav Kadam, Shan Liu, and C-C Jay Kuo. Pointhop: An explainable machine learning method for point cloud classification. *IEEE Transactions on Multimedia*, 2020.
- [10] C-C Jay Kuo, Min Zhang, Siyang Li, Jiali Duan, and Yueru Chen. Interpretable convolutional neural networks via feedforward design. *Journal of Visual Communication and Image Representation*, 60:346–359, 2019.
- [11] Min Zhang, Yifan Wang, Pranav Kadam, Shan Liu, and C-C Jay Kuo. Pointhop++: A lightweight learning model on point sets for 3d classification. *arXiv preprint arXiv:2002.03281*, 2020.
- [12] Yueru Chen and C-C Jay Kuo. Pixelhop: A successive subspace learning (ssl) method for object recognition. *Journal of Visual Communication and Image Representation*, page 102749, 2020.
- [13] Peter H Schönemann. A generalized solution of the orthogonal procrustes problem. *Psychometrika*, 31(1):1–10, 1966.